

Theoretical Mechanism for Crimp

B. N. Nagorcka

Division of Computing Research, CSIRO, P.O. Box 1800, Canberra, A.C.T. 2601.

Abstract

A mechanism for crimp in wool fibres is proposed in which the inner root sheath of the wool follicle and the fibre cuticle rotate around the fibre cortex in the region just above the follicle bulb. The rotational movement of the fibre cuticle is passed on to groups of microfibrils in the cortical cells of the fibre through a gearing action, which causes them to be twisted into helices or spirals with the result that the cortical cells tend to shorten. The fibre deforms while still in the follicle causing the position of the fibre cortex near the bulb to change. This changes the magnitude and direction of the rotational movement of the inner root sheath and cuticle. A mathematical model of the mechanism is developed and several crimp forms, produced by using the model, are compared to those commonly observed.

Introduction

The shape or form of crimp in individual fibres in wool has been described in detail by Rossouw (1931) and Chapman (1965). There appear to be three main forms:

- (1) An alternating helix (dish-shaped wave) described by Chapman (1965) as a wave 'wrapped around part of a cylindrical surface with the axis of the wave lengthwise along the cylinder'. The axis of the wave itself usually spirals slowly, so that 'the orientation of the wave...changes after the formation of several crimps (e.g. 2–8) [making] the dish-shaped wave form less obvious'. An example may be seen in Fig. 1*a*.
- (2) A helix as in Fig. 1*d*.
- (3) Uniplanar waves (Fig. 1*e*), although less frequently observed than forms (1) and (2). This form is 'more frequent in wool with a very prominent and somewhat exaggerated staple crimp' (Chapman 1965).

Changes in crimp form along a fibre are apparently commonplace (Barker and Norris 1930). For example, a helical form may suddenly change from a left-handed to a right-handed helix, or a dish-shaped wave may change to a spiral. Nevertheless, the forms described in (1), (2) and (3) above appear to be the basis of the forms observed. The mechanism for crimp proposed in this paper is capable of producing all three basic forms, but only forms (1) and (2) will be demonstrated. Form (3), in terms of the mechanism, depends on small differences in the physical properties of the ortho- and paracortex, the details of which will not be discussed.

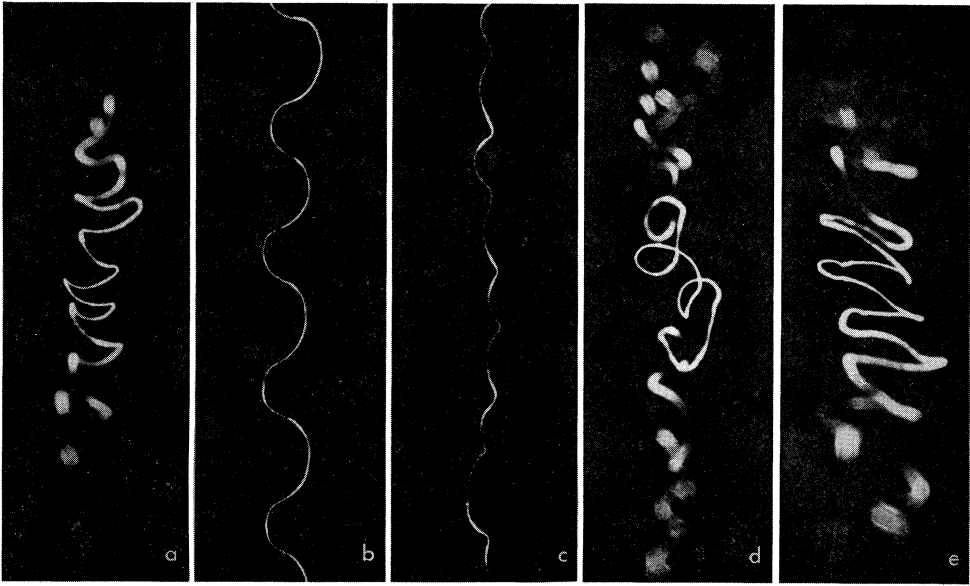


Fig. 1. Oblique longitudinal view (a), and view from above (b) and from the side (c) of the crimp form described as an alternating helix. This form is characteristic of fibres in staples of Merino wool. Oblique longitudinal view of the crimp form described as a helix (d) and of the crimp form described as uniplanar (e). [Figures reproduced by permission from Chapman (1965)].

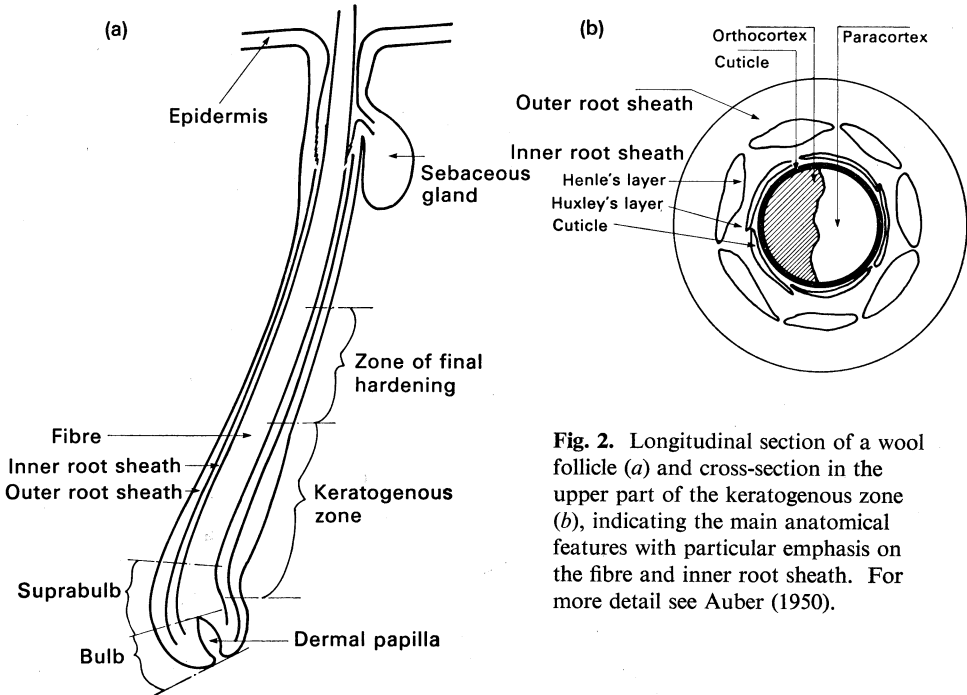


Fig. 2. Longitudinal section of a wool follicle (a) and cross-section in the upper part of the keratogenous zone (b), indicating the main anatomical features with particular emphasis on the fibre and inner root sheath. For more detail see Auber (1950).

In the past 50 years, there has been a number of models suggested to explain crimp in wool fibres. These have ranged from purely descriptive mathematical models, such as that proposed by Barker and Norris (1930), with no explanation of the mechanism responsible, to detailed physical models of the follicle, displaying the possible effects of changes in the follicle shape (Auber 1950; Mercer 1961; Chapman 1965). Chapman (1965) has listed the proposed mechanisms, emphasizing the trend which has occurred, from models in which the shape of the follicle is assumed to be the effect rather than the cause of crimp, to models where a changing follicle shape determines the crimp characteristics. The problem in the latter group of models becomes one of proposing a mechanism which causes the follicle to flex and twist; no satisfactory mechanism has ever been suggested. For example, Chapman (1965) suggested that the arrector pili musculature attached to primary follicles would cause the follicles to flex and twist. Chapman (unpublished data) has subsequently shown that follicles continue to produce crimped fibres after the arrector pili have been removed.

In this paper, a mechanism is proposed which is capable of predicting many of the observed characteristics of crimp in wool and all the observed crimp waveforms listed above. The mechanism involves feedback, since it depends on small movements within the follicle caused by crimp itself, and, therefore, cannot be strictly classed with either of the model groups mentioned above.

Outline of the Mechanism of Crimp Formation in Qualitative Terms

A longitudinal section of a wool follicle is shown in Fig. 2*a*. Mitotic activity is confined to the bulb. As the cells develop and divide they migrate up the follicle, differentiating into a number of roughly cylindrical layers referred to as outer root sheath, inner root sheath and fibre. The inner root sheath is divided further into three layers, indicated in Fig. 2*b*. The fibre consists of a cortex [plus medulla when the diameter is large enough (Auber 1950)] surrounded by the fibre cuticle. The cortex commonly consists of two hemicylinders. Although other geometrical arrangements are also found (Amad and Lang 1957), this bilateral division of the cortex into two hemicylinders is the one which is usually associated with crimp (Horio and Kondo 1953). In such a case it is known that the cells divide and develop more rapidly on one side of the bulb than on the other (Fraser 1964). It is suggested that this gives rise to a bilateral pressure distribution in the bulb with the high-pressure side being associated with the presumptive paracortex.

It is proposed that as the cells migrate out of the bulb into the region just above the follicle bulb (suprabulb) the bilateral pressure distribution, together with the geometrical asymmetry of the bulb (e.g. slightly spiral-shaped), are sufficient to cause the cells of the inner root sheath and cuticle (i.e. of both the fibre and inner root sheath) to move around the fibre cortex to some extent (Fig. 3*a*). In the distal part of the bulb and in the suprabulb the fibre cuticle cells have already flattened to a significant degree (Auber 1950). The fibre cuticle is, therefore, like a thin annular cylinder rotating about the fibre cortex. In the suprabulb the cortical cells are elongated so that they appear spindle-shaped (Auber 1950). Micro- and macrofibrils are forming within the cells and are distributed periphero-axially to a significant extent, their long axis being parallel to the presumptive fibre (Auber 1950). It is suggested that bunches of fibrils within the fibre cortex behave as 'cogged cylinders'

and that the rotational movement of the fibre cuticle is passed on to the contents of the cortical cells through a gearing action. It will be argued later that the gearing action occurs mainly at the centres of the cortical cells (because the cells are tightly joined at their ends along the long axis with neighbouring cells). The net result is that each bunch of microfibrils will be twisted into a spiral and each cortical cell will tend to shorten. In order that the paracortex should lie on the inside of the curved wool fibre, consistent with observation (Horio and Kondo 1953), it is necessary that the twisting of the microfibrils be more effective (e.g. less slippage between engaging cogs) in the para- than in the orthocortex. The paracortical cells will, therefore, tend to shorten more than the cells of the orthocortex. If this were the complete picture then the fibre, once it emerges from the skin, would deform to the shape of a true circular helix.

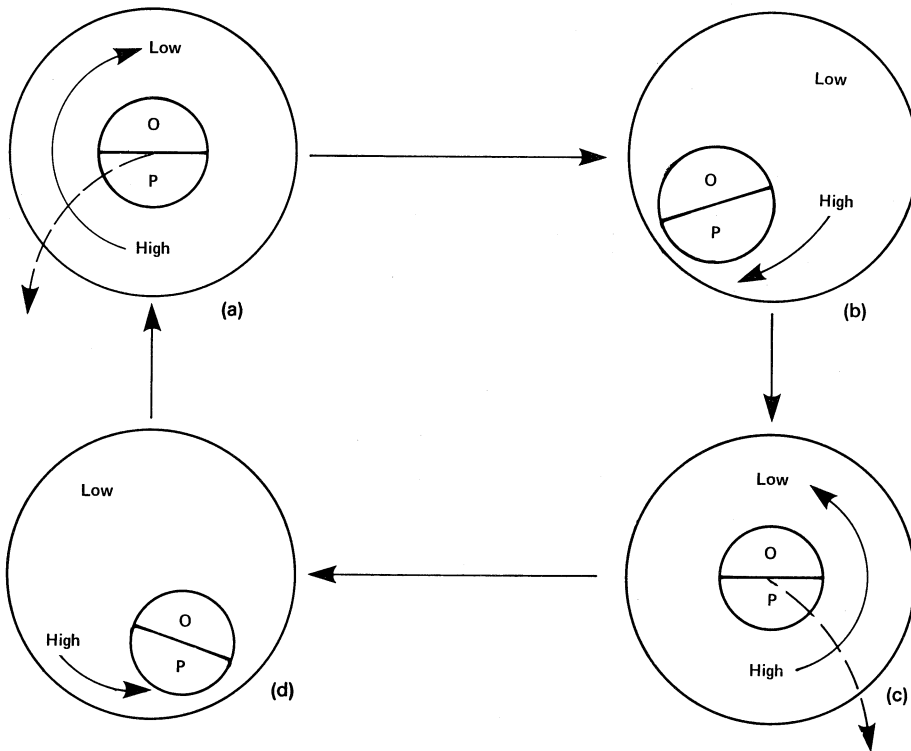


Fig. 3. Cross-sections through the suprabulb, showing the position of the fibre cortex relative to the follicle wall. The bilateral pressure distribution is indicated by High, showing the region of high pressure associated with the paracortex, and Low, the region of low pressure. The ortho- and paracortex are indicated by O and P, respectively. The rotational movement of the inner root sheath is shown as a solid arrow drawn between the high and low pressure regions in the follicle. In (a) the inner root sheath rotates clockwise. The cortical cells will eventually tend to untwist in an anticlockwise direction causing the fibre cortex to move to the lower left quadrant (b) stopping the inner root sheath movement. The pressure gradient, however, remains and an anticlockwise movement of the inner root sheath begins (c). Once this part of the fibre moves into the effective region (see text) the untwisting of the cortical cells will at first tend to offset the previous movement of the fibre and eventually drive it into the lower right quadrant (d). The anticlockwise movement of the inner root sheath is stopped while the pressure gradient, once again, remains so that conditions eventually return to the situation in 3(a).

As the fibre develops and moves up the follicle, however, the stresses induced in the fibre in the suprabulb cause the fibre to deform slightly while still in the follicle. This sets off a sequence of events which repeats itself over and over again. The fibre, tending to deform to a helix while still in the follicle, forces the fibre cortex in the suprabulb to move over to the side of the follicle (Fig. 3*b*). This reduces the rotational movement of the inner root sheath and cuticle, which is the cause of the tendency to deform, and eventually stops it. The bilateral pressure distribution remains, however, so that the inner root sheath and cuticle in the suprabulb begin to rotate in the opposite direction around the fibre (Fig. 3*c*). (A more complete description of these events is given later.) The fibre now being formed, once it reaches the upper part of the follicle, will tend to deform to a helix of opposite direction (e.g. a left-handed instead of a right-handed helix). This causes the fibre cortex in the suprabulb to move away from the side of the follicle towards the opposite side where, once again, it stops the rotational movement (Fig. 3*d*). The rotational movement begins again in the opposite direction, returning the situation to the point as indicated initially in Fig. 3*a*. The fibre which now emerges will tend to deform to an alternating helix, i.e. a helix which keeps reversing its direction [see Introduction, form (1)].

There is a third factor which must be taken into consideration. In general the follicle bulb is not only deflected as shown in Fig. 2*b*, but curves slightly so that it tends to spiral. It is suggested that a spiral-shaped bulb will cause the rotational movement of the inner root sheath to be greater in one direction than in the other, leading to an alternating helix which rolls either slowly [see the description of form (1)] or more rapidly, depending on the degree to which the follicle bulb itself spirals. If the bias introduced by the spiral shape of the bulb is great enough so that the rotational movement never reverses, then the fibre which emerges will deform to a distorted helix [form (2)], an example of which will be given later.

The mechanism, as outlined above, is based upon a series of assumptions, as follows:

- (1) There is a net rotation of the inner root sheath and cuticle about the fibre cortex in the region of the suprabulb.
- (2) The rotational movement of the fibre cuticle in the suprabulb region is passed on to the elongated cortical cells and the microfibrils contained within them, through a gearing action in which bunches of microfibrils, known to be aligned to a significant extent with the axis of the fibre (Auber 1950), act as if they are 'cogged cylindrical gears'. The 'gears' are envisaged as extending nearly the full length of the cell.
- (3) The gearing action is confined mainly to the centres of the cortical cells. A small amount of twisting of the lower ends of the cells relative to the upper ends about the axis of the fibre also occurs.
- (4) The gearing action is more effective in the cells of the paracortex than of the orthocortex.
- (5) Young's modulus for both the inner root sheath and fibre increases with distance up the follicle.
- (6) The net rotational movement, K , adjusts towards its equilibrium value, K_e , at a rate proportional to the difference $K - K_e(P)$, where K_e depends on the position (P , defined later) of the fibre cortex relative to the follicle wall.
- (7) The modulus of K_e is not altered by the movement of the cortex near the bulb.

It is envisaged that the rotational movement is concentrated in the cylindrical layers of cells making up the inner root sheath and cuticle [cf. assumption (1)] but there may well be differential movement between layers. Differential movement of cell layers up the follicle has been observed in wool follicles (Chapman 1971).

In the examples discussed later the total net rotational movement of the fibre cuticle *relative* to the fibre cortex, denoted by K , is assumed to be 0.4 rad or about one-sixteenth of a full rotation. In the mathematical model this has been found to be sufficient to produce the observed crimp forms.

In summary the consequences of the rotational movement are as follows:

- (1) Internal shear and longitudinal stresses will be induced in the cells of the cortex through the twisting of groups of microfibrils into 'spirals'.
- (2) The fibre will bend and twist to some extent while still in the follicle in response to the internal stresses within the fibre.
- (3) Any bending and twisting of the fibre within the follicle will cause the position of the fibre cortex relative to the follicle wall in the suprabulb region to change.
- (4) A change in the relative position of the fibre in the suprabulb region will cause a change in the magnitude and perhaps the direction of the net rotational movement of the inner root sheath and cuticle cells in this region.

These effects constitute a feedback loop since any change in the magnitude of the rotational movement (4) will cause a change in the magnitude of the internal shear and longitudinal stresses induced in the cells of the cortex (1). The consequences (1)–(4) will now be discussed in detail and a quantitative description of the mechanism will be developed.

A Mathematical Model of the Mechanism

Glossary of Symbols

Symbol	Unit	Meaning
i		Subscript; $i = o, p, m$ denotes orthocortex, paracortex or matrix, respectively
A	(rad)	Angle of pitch of a circular helix formed by the fibre
a	(rad)	Angle of pitch of a circular helix formed by microfibrils within the cortical cells
A_i	(mm ²)	Cross-sectional area of fibre component $i = o, p$
C_p		Crimp prominence defined as the straight fibre length divided by the relaxed fibre length, i.e. length of the crimped fibre
D	(mm)	Fibre diameter
d	(mm)	Diameter of a 'cylinder' of microfibrils characteristic of cell type
E_i	(g day ⁻² mm ⁻¹)	Young's modulus of fibre component $i = o, p$; it is often assumed in the paper that $E_o = E_p = E$
f		Rotational movement which causes twisting of the cortical cells about the fibre axis is expressed as a fraction f of $K(t)$
g_i		Effectiveness of gearing action in cortical cell, $i = o, p$
$K(t)$	(rad)	Net rotational movement of the fibre cuticle relative to the fibre cortex, which in general changes with time t
$K_e(P)$	(rad)	Equilibrium value of $K(t)$ which depends on $P(t)$
K_0	(rad)	Constant used to define K_e as a function of $P(t)$ —cf. equation (13)
K_s	(rad)	Bias in the value of $K_e(P)$ due to the spiralled shape of the follicle bulb—cf. equation (17)
L_f	(mm)	Follicle length
L_1	(mm)	Distance up the follicle at which fibre curvature begins to affect $P(t)$
L_2	(mm)	Distance up the follicle at which fibre curvature ceases to affect $P(t)$

<i>Symbol</i>	<i>Unit</i>	<i>Meaning</i>
L_i	(g mm ² day ⁻²)	Torque arising from fibre components $i = o, p, m$
l	(mm)	Length of cortical cell
Δl	(mm)	Change in length of cortical cell due to twisting of microfibrils
M_i	(mm ⁴)	Second moments of area of fibre component $i = o, p, m$ about the centre of the fibre
$P(t)$		Quantity of arbitrary scale indicating the position of the fibre cortex relative to the follicle wall in the suprabulb region, as a function of time, t
R	(mm)	Radius of curvature of the fibre
R_h	(mm)	Radius of curvature of a circular helix formed by the fibre
$r(t)$	(mm)	Crimp form produced in three-dimensional space
t	(days)	Time defined so that $t = 0$ at the time the tip of the fibre, above the skin surface, was being formed
T	(days)	Period of oscillation in $K(t)$ and $P(t)$
v	(mm day ⁻¹)	Fibre length growth rate
z	(mm)	Distance up the follicle measured from the base of the bulb
α^*		Arbitrary constant used to defined $P(t)$
β^{-1}	(days)	Time constant for a change in $K(t)$, i.e. time required for $K(t)$ to move two-thirds of the way towards a new equilibrium value
δ_m	(rad mm ⁻¹)	Angle of twist of hardened fibre per unit fibre length
δ_i	(rad mm ⁻¹)	Effective angle of twist per unit fibre length remaining in the hardened fibre component $i = o, p$
ϵ_i		Longitudinal strain in fibre component $i = o, p$ due to twisting of macrofibrils
Φ	(rad)	If $r(t)$ traces out a circular helix in the z -direction, then Φ is the phase angle of the point $r(t)$ on the circle in the xy -plane
μ_i	(g day ⁻² mm ⁻¹ rad ⁻¹)	Shear modulus of fibre component $i = o, p, m$

Induction of Stress in the Cortical Cells [Assumption (2)]

Rogers (1959a) has observed that cortical cells 'interdigitate with adjacent cells' through 'finger-like processes' at their ends. The drawings of cortical-cell packing by Auber (1950) suggest that this process is already beginning in the suprabulb through corrugation or convolution of cell membranes at the ends of the cells, as shown in Fig. 4a. Mercer (1961) regards this type of 'interdigitation of confronted membranes' as indicative of strong adhesion and states that 'desmosomes (tight junctions between cell membranes) usually form on such surfaces to add to the adhesion'. It follows that cortical cells in the suprabulb must be tightly joined, at their ends along the long axis, with cells above the suprabulb where no rotational movement of the fibre cuticle and inner root sheath occurs. The lengthwise joining of the cortical cells with neighbouring cells (Fig. 4a) would, therefore, tend to prevent the cortex in the suprabulb region from being rotated as a whole. The extent to which the fibre cortex does rotate with the fibre cuticle is, by definition, not included in K . The proposed gearing action [assumption (2)], however, could occur, but would be confined mainly to the central regions of the cells as indicated in Fig. 4a. Some twisting of the lower ends of the cells relative to the upper ends about the axis of the fibre is also required. It is assumed later that the lower ends of the cells are twisted 0.12 rad (7°) about the fibre axis, in order to explain the twisting observed in the hardened fibre.

The results presented in this paper suggest that about one-quarter of a turn by the cortical cells at their centres may be sufficient to produce the observed crimp

waveforms. Some breaking of desmosomes at the centres of the cells, where the torque is greatest, may be necessary. Chapman and Gemmell (1971) have observed broken desmosomes in the suprabulb region.

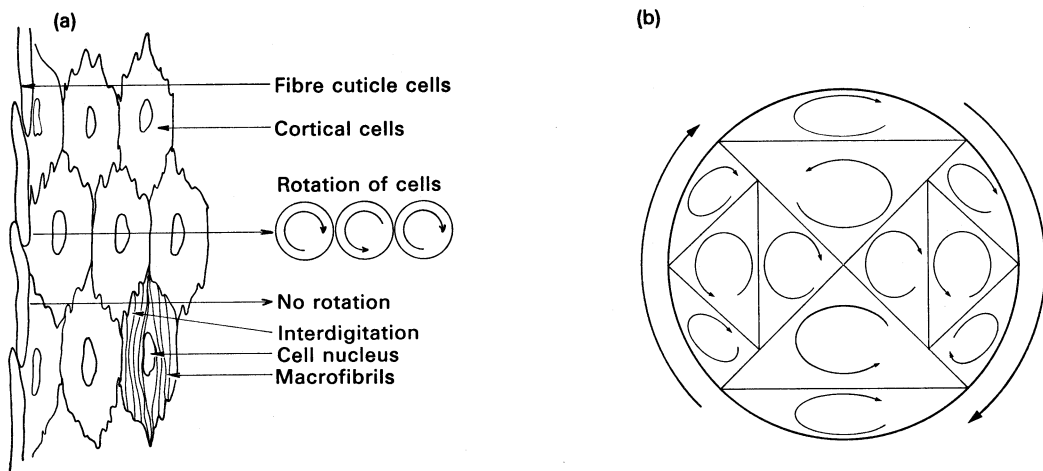


Fig. 4. (a) Idealized cortical-cell packing arrangement as seen in a longitudinal section of the fibre near the follicle bulb. It may be compared with those observed by Auber (1950, Fig. 12). The fibre cuticle is assumed to be rotating into the plane of the diagram. The effect of this in rotating the central regions of the cells through a gearing action is shown in two dimensions. (b) Cross-section through the centres of the cortical cells, showing a regular two-dimensional packing arrangement with no voids, in which no cell membrane moves counter to its neighbour. The direction of rotation of each cell and the fibre cuticle is indicated.

Gearing Action [Assumptions (3) and (4)]

The effect of the gearing action [cf. assumption (3)] is to twist the cylinders of microfibrils, causing cylindrical layers of microfibrils to spiral. This is consistent with the observations of Rogers (1959*b*) who attributes the 'whorly' appearance of macrofibrils in the orthocortex of wool fibres to spiral-type packing of the microfibrils. It is also tempting to suggest that the twisting may, in part, cause 'macrofibrils adjacent to the cell boundaries in the paracortex to develop into contiguous masses' and in the orthocortex to cause the macrofibrils to be 'predominantly circular in cross-section and build up as discrete bundles' as observed by Chapman and Gemmell (1971). These suggestions could be tested by comparing the structure of cells not influenced by a rotational movement of the inner root sheath (it is shown later in the paper that such a situation does occur in a predictable fashion) with those which are.

An example of a two-dimensional packing arrangement of cells across the fibre, in which no cell membrane moves counter to its neighbour, is shown in Fig. 4*b*. In reality the packing arrangement is not regular and at least part of some membranes will be required to move in the opposite direction from neighbouring membranes. If there is sufficient energy associated with the rotational movement of the inner root sheath and fibre cuticle, either the opposing cell membranes will be forced to break contact with each other or groups of cortical cells will be forced to move about each other until a packing arrangement which is stationary with respect to

the gearing action is reached, or both will occur. Some of the rotational movement of the fibre cuticle may therefore be ineffective in causing the microfibrils to twist. This ineffective part of the rotational movement is, by definition, not included in K .

Consider a group of microfibrils forming a 'cylinder' of diameter d which is characteristic of other groups within the cell. Let the fibre diameter be D . The fibre cuticle undergoes a net rotation of K rad while in the suprabulb, the sign of K specifying the direction of rotation. Ignoring any twisting at the ends of the cell the number of twists in the helical structure between the centre and the end of the cell is $D|K|/2\pi d$. The cortical cells of length, l , will tend to shorten by a distance Δl and translate the torque causing the twisting into a longitudinal strain given by $\Delta l/l$. The expression for Δl is

$$\Delta l = D|K|g,$$

where

$$g = (1 - \sin a)/\cos a. \quad (1)$$

The expressions for Δl and g are based on relationships between the length (l), axial length, diameter (d) and angle of pitch (a) of a circular helix. The parameter g , which has a value between zero and one, will be referred to as the effectiveness of the gearing action since it specifies the fraction of the maximum amount of shortening theoretically possible ($D|K|$) which occurs for a given rotational movement K . In general g will depend on other factors besides the angle of pitch a . The effect of any slippage between 'cylinders' involved in the gearing action, for example, should be included in g .

If the proposed gearing action is responsible for the observed microfibril structure (Auber 1950; Rogers 1959b), in the orthocortex d would correspond to the diameter of macrofibrils characteristic of the orthocortex while in the paracortex d would have a value close to the diameter of the paracortical cells. The fibrillary structure would then be consistent with the 'whorls' seen in the orthocortex compared with the linear structure seen in the paracortex (Rogers 1959b). With this interpretation of the observations it seems reasonable to expect that the effectiveness of the gearing action in the paracortex (g_p) will be different from that of the orthocortex (g_o). If g_p is greater than g_o , Δl will be greater in the para- than in the orthocortex, causing the paracortex to lie on the inside of the curved fibre, consistent with observation (Horio and Kondo 1953). Significant structural differences have been observed (Chapman 1976) between cells of the ortho- and paracortex in the suprabulb which could lead to a difference in the effectiveness of the gearing action in the two cell types. It seems reasonable to assume therefore that the gearing action is more effective in the cells of the paracortex than in the orthocortex [i.e. assumption (4)].

Deformation of the Fibre

As the cells of the fibre cortex move through the upper half of the keratogenous zone (Fig. 2a) it has been observed (Chapman 1976) that the matrix, an amorphous component which develops between the micro- and macrofibrils, forms simultaneously with the microfibrils in both the para- and orthocortical cells. At a later stage disulfide bonds are formed, cross-linking the polypeptide chains of keratin which tend to be aligned with the axis of the fibre (Onions 1962). This is part of the process of hardening (Fig. 2a). The twisted microfibrils are now embedded in an amorphous 'elastic cement', i.e. the matrix.

As a first step in determining the deformation of the fibre within the follicle the effect of the longitudinal and shear stresses on the completed fibre alone will be considered. Once free of the constraint of the follicle, the microfibrils of the cortical cells will tend to untwist and release the stresses originally induced in the follicle bulb. The matrix prevents a reversal of most of the original movement of the fibre cuticle and the associated gearing action. Some release of the induced stresses, at least from those cells twisted about the fibre axis, can be achieved by twisting the completed (hardened) fibre. The shape of the deformed fibre may be estimated by considering the longitudinal and shear stresses separately. The shear stress provided by the cross-linking associated with the matrix (other factors such as the fibre cuticle should also be included; however, only the matrix will be referred to here) must balance the shear stress arising from the twisted microfibrils of the ortho- and paracortical cells. Let δ_m be the amount by which the fibre twists per unit length before equilibrium between the cortical cells and the matrix is reached. δ_o and δ_p are the effective angles of twist about the fibre axis per unit fibre length which still remain in the ortho- and paracortex, respectively, following the untwisting. A_p , μ_p , A_o , μ_o , and A_m , μ_m are the cross-sectional area and shear moduli of the para-, orthocortex and hardened matrix, respectively. In equilibrium the torque L_m , L_o and L_p in these three components must balance, i.e. $L_m = L_o + L_p$. From the relationship between shear stress and shear strain for a twisted cylinder it follows that the torque for each component is given by

$$L_i = \int r_i \delta_i \mu_i r_i dA_i, \quad i = o, p, m,$$

hence

$$\mu_m M_m \delta_m = \mu_p M_p \delta_p + \mu_o M_o \delta_o, \quad (2)$$

where

$$\delta_m + \delta_i = fK/l, \quad i = o, p. \quad (3)$$

fK is the rotational movement which caused twisting of the cortical cells about the fibre axis, expressed as a fraction, f , of K . M_i are the second moments of area of each component about the centre of the cylinder (fibre). An expression for δ_m in terms of K may be obtained by substituting equation (3) into equation (2):

$$\begin{aligned} \delta_m &= [(\mu_p M_p + \mu_o M_o)/(\mu_p M_p + \mu_o M_o + \mu_m M_m)] \cdot (fK/l) \\ &= \mu_R \cdot fK/l. \end{aligned} \quad (4)$$

μ_R is a ratio involving the shear moduli of various components of the fibre and the second moments of area over which they are distributed.

The longitudinal strains cause the fibre to bend with curvature R^{-1} . An expression for R in terms of the mechanical properties of the fibre has been derived in the Appendix. If it is assumed, for the sake of simplicity, that Young's modulus for the ortho- and paracortex, denoted E_o , E_p , respectively, are equal and that the fibre has circular cross-section with $A_p = A_o$, then

$$R = 3\pi D/16(\varepsilon_p - \varepsilon_o). \quad (5)$$

ε_p and ε_o are the longitudinal strains in the para- and orthocortex of the emerged fibre. They may be expressed in terms of K using equation (1):

$$\varepsilon_i = D|K|g_i/l, \quad i = o, p \quad (6)$$

Substituting equations (6) and (3) in equation (5) produces the following relationship for R :

$$R = 3\pi l/16|K|(g_p - g_o). \quad (7)$$

Equations (4) and (7) relate the twisting, δ_m , and curvature, R^{-1} , at a point x , say, along the fibre to the physical properties of the fibre at x and the net rotational movement, K , of the inner root sheath and cuticle, which occurred at the time that the part of the fibre at x was being formed. If the physical properties and K remain unchanged with time then the deformation shape of the fibre would be a circular helix with angle of pitch, A , and radius R_h where

$$R_h = R \cos^2 A, \quad (8)$$

$$A/\cos A = \pi R \delta_m/2. \quad (9)$$

These equations can be obtained using formulae describing a circular helix (cf. Thomas 1962). Substituting for R and δ_m in equation (9) from equations (7) and (4) would show that the right-hand side of equation (9) depends on the sign of K and is independent of its magnitude. If the sign of K changed then the helix would appear to suddenly change from being right-handed, for example, to left-handed.

In general the fibre at each point along its length, both within and outside the follicle, will tend to deform to a helical shape with the angle of pitch and the radius of curvature determined by the net rotational movement which influenced the development of the fibre at that point [see equations (7), (8) and (9)]. The degree to which the fibre within the follicle actually deforms will be strongly influenced by the elastic properties of the follicle itself.

Relative Position of the Fibre Cortex near the Bulb [cf. Assumption (5)]

The curvature and twisting of the fibre within the follicle will determine the position of the fibre cortex, relative to the follicle wall near the bulb. Since the fibre tends to deform to a helical shape within the follicle the cortex near the bulb will tend to move into one of two adjacent quadrants as shown in Fig. 3. For the purposes of the mathematical model it is not necessary to know the precise position. A quantity $P(t)$ is introduced as an indicator of the position of the cortex near the bulb at time t . P is proportional to the expected displacement of the follicle bulb due to curvature of the fibre within the follicle:

$$P(t) = \alpha^* \int_0^{L_f} \text{sgn } K/R(z) dz.$$

α^* is a constant, L_f is the follicle length and z ranges between zero at the base of the bulb and L_f at the skin surface. Using equations (A5) and (A6) (Appendix), which include the effects of the inner and outer root sheaths, to substitute for $R(z)$ and making use of equations (6) and (3) it follows that

$$P(t) = \alpha^* \int_0^{L_f} G(z) K[t - (z/v)] F(z) dz,$$

where

$$G(z) = E(z) u_p A_p D(g_p - g_o)/2l,$$

and

$$F(z) = [E(z)(I_o + I_p) + E_{irs}(z)I_{irs} + E_{ors}I_{ors}]^{-1}.$$

E , E_{irs} and E_{ors} are Young's moduli for the fibre, inner root sheath and outer root sheath, respectively, and u_p , I_o , I_p , I_{irs} and I_{ors} are defined in the Appendix. v is the length growth rate of the fibre. Time, t , is defined such that t is zero at the time the tip of the emerged fibre was being formed in the follicle bulb. The sign of P determines in which of the two quadrants the cortex is located. The magnitude of P gives the distance of the cortex from the follicle centre.

Assumption (5) seems reasonable for the inner root sheath since it is known that hardening of the inner root sheath increases with distance from the follicle bulb (Auber 1950). The effect of various stages of keratinization on Young's modulus for the fibre is not known, although hardening of the fibre also increases with distance from the bulb. In addition, if the moisture content of bulb cells is similar to that of other tissues at about 80% and the maximum moisture content of keratinized fibre cells (i.e. at 100% R.H.) is 33% (Onions 1962), it follows that the water content of the fibre must decrease as it moves up the follicle. Young's modulus is known to increase in wool fibres with decreasing water content (Onions 1962).

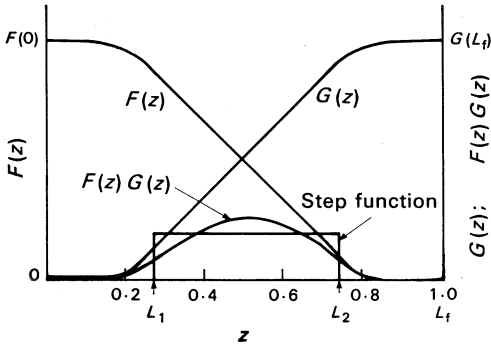


Fig. 5. Example of the functions $F(z)$ and $G(z)$, defined in the text, and their product as a function of the distance, z , from the follicle bulb. z is plotted on the horizontal axis as a proportion of follicle length, L_f . The product $F(z)G(z)$ is compared to a step function.

Assumption (5) has the consequence that function $F(z)$ in the definition of $P(t)$ will decrease with distance, z , from the follicle bulb. $G(z)$ on the other hand will increase. A possible example of the functions $F(z)$ and $G(z)$ and their product is shown in Fig. 5. Only the values of K associated with position along the fibre between L_1 and L_2 would significantly influence P in this case suggesting that P might well be approximated by the less complicated expression:

$$P(t) = \alpha \int_{L_1}^{L_2} K[t - (z/v)] dz, \quad (10)$$

where α is a constant. This is equivalent to using a step function, shown in Fig. 5, as the weighting function of K . Equation (10) may also be written in the differential form,

$$dP(t)/dt = \alpha v \{K[t - (L_1/v)] - K[t - (L_2/v)]\}. \quad (11)$$

In this form the equation becomes one of the model equations summarized later.

In the previous section it was shown that at each point along the fibre, the tendency is to deform to either a left-handed or a right-handed helix depending on the sign of K . Since the paracortex is always on the concave side of the curvature the expected

relative movement of the cortex near the bulb is illustrated in Figs 3*a* and 3*b*. At the stage shown in Fig. 3*a* the rotational movement of the inner root sheath is such that untwisting of the cortical cells, once they pass into the effective region between L_1 and L_2 , will cause the relative position of the presumptive cortex to move in the direction indicated by the dashed arrow. The cortex, therefore, moves in such a way that K is reduced and finally reversed. This is shown quantitatively in a later section when the model equations are summarized and solved. The eventual position of the cortex may be only slightly off-centre. Non-central positioning of the cortex near the bulb is observed (Auber 1950) in follicles containing deflected bulbs.

Magnitude and Direction of the Net Rotational Movement [Assumptions (6) and (7)]

The fluid dynamical problem concerning the viscous compressible flow of developing cells out of the bulb through the suprabulb region and up the follicle is a formidable one. No attempt will be made here to consider the complexities of this problem. Instead only the magnitude and direction of the postulated net rotational movement will be quantified on the basis of assumptions (6) and (7).

Assumption (6) simply asserts that there is a finite time required for the net rotational movement to adjust to any changes in the factors which cause it. The adjustment is assumed to be a very simple one which may be written mathematically as:

$$dK(t)/dt = -\beta[K(t) - K_e(P)], \quad (12)$$

where β is a constant.

In view of the discussion concerning assumption (1), assumption (7) may be considered equivalent to assuming that the mitotic activity in the bulb and the asymmetrical shape of the bulb remain unaltered by the changing position of the fibre cortex near the bulb. Assumption (7) states that the modulus of K_e is a constant, leaving only the sign of K_e to be determined. The sign of K_e was deduced on the basis that the fibre, contained in the follicle, will deform to a helical shape with the paracortex on the concave side of the curvature as discussed in the previous section. In forming the helix the fibre tends to twist in the reverse direction to the K which induced the shear and longitudinal strains. The effect on the cortex near the bulb is shown in Fig. 3. If the rotational movement of the inner root sheath is clockwise, as in Fig. 3*a*, the cortex will eventually be forced to move into the lower left quadrant (Fig. 3*b*). This will have the effect of reducing K , which is represented by changing the direction of K_e since the bilateral pressure distribution and bulb asymmetry remain. K begins changing direction and is ultimately reversed (Fig. 3*c*). As K reduces and changes sign the cortex eventually (i.e. once the effect of the change passes into the sensitive region between L_1 and L_2) moves back to the centre (Fig. 3*c*) and continues to move into the lower right quadrant (Fig. 3*d*). K_e is reversed, once again, since the rotational movement of the inner root sheath will be affected. The cortex will eventually move back to its original position (Fig. 3*a*) and the inner root sheath will be moving in a clockwise direction. Clearly Fig. 3 summarizes a feedback mechanism which is at the core of the proposed mechanism for crimp. If P is defined to be positive in the lower left quadrant (and negative in the lower right quadrant), K_e is defined as follows:

$$K_e = \begin{cases} -K_0, & P > 0 \\ +K_0, & P < 0 \end{cases} \quad (13)$$

Model of Crimp Mechanism

The proposed crimp mechanism may now be summarized in the form of a mathematical model:

$$dP(t)/dt = \alpha v \{K[t - (L_1/v)] - K[t - (L_2/v)]\}, \quad (11)$$

$$dK(t)/dt = -\beta [K(t) - K_c(P)], \quad (12)$$

$$\delta_m = \mu_R \cdot f K/l, \quad (4)$$

$$R = 3\pi/16 |K|^\gamma [g_p^\gamma - g_o^\gamma], \quad (14)$$

$$R_h = R \cos^2 A, \quad (8)$$

$$A/\cos A = \pi R \delta_m/2. \quad (9)$$

Equation (14) was obtained from equation (5) and substituting

$$\varepsilon_i = D(|K|g_i)^\gamma/l, \quad i = p, o$$

which, if $\gamma \neq 1$, introduces a non-linear relationship between longitudinal strain and degree of effective twisting, emphasizing that equation (1) is an approximation. Non-linear stress-strain relationships are frequently observed and wool is one substance for which a non-linear relationship has been observed (Onions 1962). The non-linearity is introduced here to make the angle of pitch, A , depend to a small extent on K . For $\gamma > 1$, A will pass through $\pi/2$ as K decreases and changes sign allowing a smoother transition for a change in direction of the helix than would be the case for $\gamma = 1$.

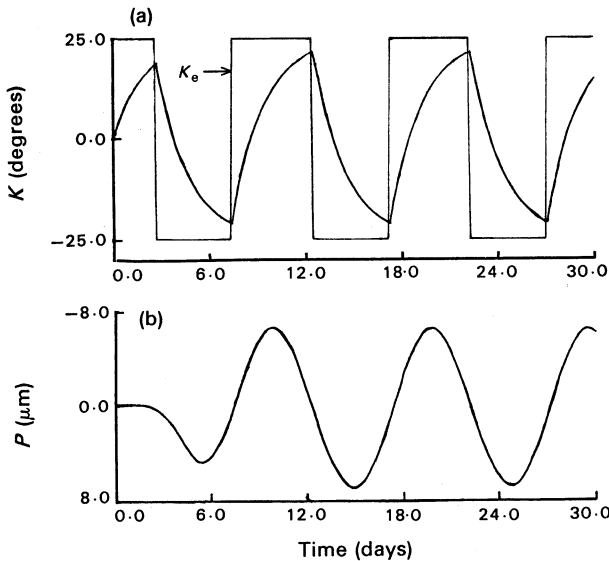


Fig. 6. Equations (11) and (12) were solved using the parameter values in Table 1. K was initially set to zero and P to a very small positive value. Both P and K have been plotted as a function of time. $K_c(P)$ is also shown. The small perturbation given to P has caused both P and K to oscillate.

The set of equations listed above will, in general, define a different helix at each point of time. Therefore, the following equations, which may be obtained from the analytical description of the helix, are needed to complete the model:

$$dr(t)/dt = v[-\cos(A)\cos(\Phi)\mathbf{i} + \cos(A)\sin(\Phi)\mathbf{j} + \sin(A)\mathbf{k}] \operatorname{sgn}(K), \quad (15)$$

$$d\Phi/dt = (\cos(A)v/R_h)\text{sgn}(K), \quad (16)$$

where the vector $r(t)$ is the crimp form produced in three-dimensional space, and i , j and k are unit orthogonal vectors along the x , y and z axes in a rectangular coordinate system. If $r(t)$ traces out a circular helix such that the axis of the helix corresponds to the z -axis then the point $r(t)$ in the xy -plane will trace out a circle with time. Φ is the angle between the point $r(t)$ in the xy -plane and $-j$ and will be referred to as the phase of the helix. In general the procedure is to first solve for K using equations (11) and (12) and then to evaluate equations (4), (14), (9), (8), (15) and (16) in sequence and obtain the crimp form given by $r(t)$. Several examples are discussed in the next section.

Table 1. Model parameter values used to obtain the results discussed in the text, unless stated otherwise

Parameter	Value	Comments
α	2×10^{-4}	Arbitrary; set to constrain P , $-10 \mu\text{m} < P < +10 \mu\text{m}$
β	0.5 day^{-1}	N.d. ^A
L_t	2 mm	Typical value (Nay and Johnston 1967)
L_2	0.5 mm	$L_2 < L_1 < L_t$ ^A
L_1	1.5 mm	
v	0.3 mm/day	Typical value (Downes and Sharry 1971)
μ_R	0.8	$0 < \mu_R < 1$ ^A
g_p	0.4	N.d. ^A
K_0	0.412 rad (24°)	These three parameters set to obtain $-\pi/2 < \Phi < \pi/2$, $C_p = 1.4$ and $R^{-1} \cong 1.5 \text{ mm}^{-1}$ (see text), with the constraint $g_o < g_p$
f	0.35	
g_o	0.1	
γ	1.1	Set to be slightly greater than 1, for reasons discussed in text.
l	0.1 mm	Typical value (Brown and Onions 1961)

^A No data are available on the basis of which an estimate of the parameter can be made.

Equations (11) and (12) contain the feedback mechanism which is essential for crimp. While $P = 0$, $K = 0$ is a solution to these two equations, it is unstable and a slight perturbation will cause both P and K to oscillate as shown in Fig. 6. The results in Fig. 6 were obtained by solving equations (11) and (12) numerically using the parameter values given in Table 1.

It is possible to obtain an approximate analytical solution to equations (11) and (12) by using the describing-function method, as described, for example, by Jacobs (1974). It is intended to present the details of this method as part of another paper. In particular it is possible to derive algebraic expressions for both the period, T , and amplitude of oscillation in P . Once T is known equation (12) may be solved with the result

$$K(t) = \begin{cases} -K_0 + K_1 \exp(-\beta t), & 0 < t < T/2 \\ K_0 - K_1 \exp[-\beta(t - T/2)], & T/2 < t < T \end{cases}$$

where

$$K_1 = 2K_0/[1 + \exp(-\beta T/2)].$$

Some of the parameter values in Table 1 are based on direct experimental observations and these have been indicated. There are other indirect observations which also help to constrain some of the values of these parameters: C_p , the ratio of straight length to relaxed or crimped length (referred to as crimp prominence by the present author—see also Rossouw 1931; Balasubramaniam and Whiteley 1964), fibre curvature,

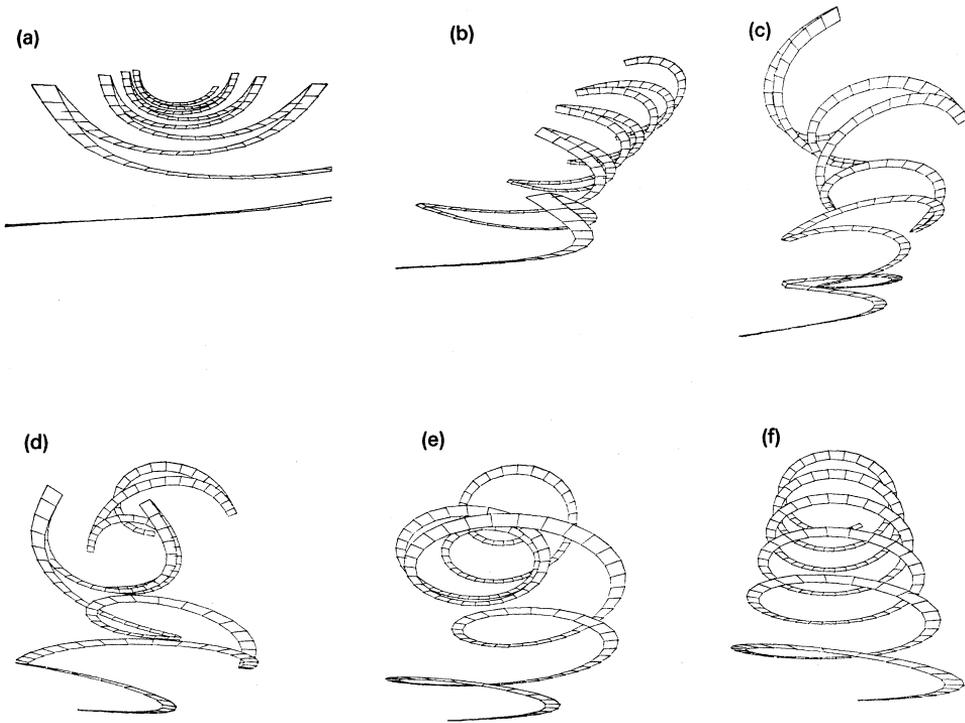


Fig. 7. All diagrams correspond to three-dimensional views of a ribbon cut from a fibre $50\ \mu\text{m}$ in diameter. The fibre is assumed to consist of two hemicylinders, one corresponding to the paracortex and the other to the orthocortex. The ribbon has been taken through the centre of the fibre, at right angles to the join of the two hemicylinders. (a) Alternating helix crimp form produced using the parameter values in Table 1. If a bias K_s in the rotational movement is introduced the plane of the crimp form in (a) rotates as seen in (b), (c) and (d) for $K_s = 2^\circ$, 5° and 10° , respectively. If the bias dominates the rotational movement, e.g., $K_s = 40^\circ$ and $K_o = 10^\circ$, then the result is a helical crimp form seen in (e) which may be compared with a true circular helix ($K_s = 40^\circ$ and $K_o = 0^\circ$) shown in (f).

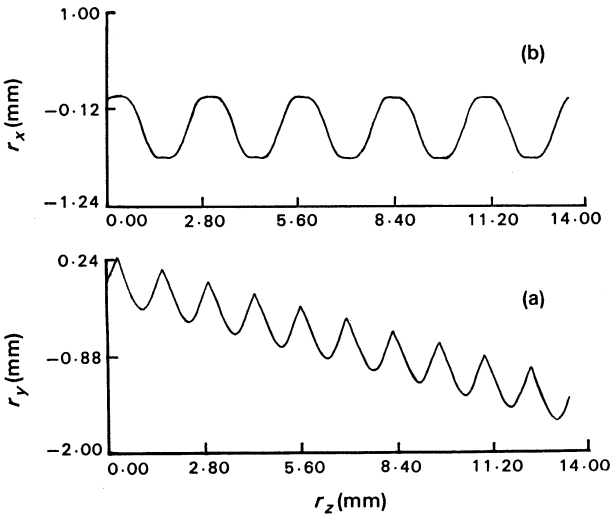


Fig. 8. Side view (a) and top view (b) of the alternating helix crimp form in Fig. 7a, obtained using the parameter values in Table 1 substituted in equation (15).

R^{-1} (Brown and Onions 1961), and measurements of Φ (Rossouw 1931), defined in equation (16). Assuming that $g_p = 0.4$, then values for g_o , μ_R and K_0 in Table 1 were chosen so that $C_p = 1.4$, $R^{-1} = 1.5 \text{ mm}^{-1}$ and $-\pi/2 < \Phi < \pi/2$, which are typical of observations.

Results and Discussion

When the model equations (listed in the previous section) are solved using the values of parameters listed in Table 1 the result is an alternating helical crimp form (i.e. class 1, described in the Introduction). This is shown in Fig. 7a when viewed along the axis (approximately) of the cylinder. The form when viewed from the top and side is shown in Fig. 8. These results should be compared with Figs 1a, 1b and 1c. The phase of the alternating helix, Φ , ranges between $\pm\pi/2$, consistent with the measurements of Rossouw (1931). When viewed from above (Fig. 8b) the form appears to approximate a series of semicircles (the horizontal scale is 2.5 times the vertical scale in Fig. 8) and compares well with that observed (Fig. 1b). The side view (Fig. 8a) shows a series of sharp peaks separated by smooth troughs which once again is in very good qualitative agreement with observation (Fig. 1c). The falling away of the fibre in this plane of view in theory (Fig. 8a) is due to the asymmetry of the oscillation of K with respect to a reversal in time, i.e. $K(t' + t) \neq K(t' - t)$, where $K(t')$ is a maximum or minimum of $K(t)$ occurring at time t' (see Fig. 8). If $K(t)$ were a trigonometric function, of time for instance, no such falling away would be observed.

It is more usual (Chapman 1965) to find that the plane of the alternating helical form rotates every two to eight crimps (Fig. 1a). This can be achieved within the present model by introducing a bias, K_s , into the definition of $K_c(P)$ as follows:

$$K_c(P) = \begin{cases} -(K_0 + K_s), & P > 0 \\ K_0 + K_s, & P < 0 \end{cases} \quad (17)$$

The crimp form obtained for several increasing values of K_s are shown in Figs 7b, 7c and 7d. The 'rolling' effect of K_s is clearly visible. The interpretation of K_s is that it corresponds to the degree to which the follicle spirals in the suprabulb region. In such a case it seems reasonable to expect that the inner root sheath will be forced, due to friction, to rotate to some extent about the axis of the follicle. The direction of rotation would be determined by the spiral shape of the follicle near the suprabulb. If there is also a bilateral segmentation in the pressure distribution, within the bulb, it follows that the proposed rotational movement of the inner root sheath will be biased by the spiral shape in a manner which is described by equation (17). The results in Figs 7b, 7c and 7d, therefore, suggest that the rotating plane of the alternating helical waves is the direct result of a spiral-shaped follicle.

If the bias introduced by the shape of the follicle dominates the variation in the rotational movement caused by the feedback mechanism then a helical or class-2 crimp form will result. Two examples of helical or class-2-type crimp forms were obtained (Figs 7e and 7f) by setting $K_0 = \pi/18$, $K_s = \pi/4.5$ and $K_0 = 0$, $K_s = \pi/4.5$. A zero value for K_0 results in a true helix (Fig. 7f) but a non-zero value causes the axis of that helix to move along a curved, perhaps helical, path (Fig. 7e).

These results suggest that deflected bulbs produce class-1 forms and spiralled bulbs produce class-2 forms, which is consistent with the statement by Wildman (1932)

that 'the shape of the basal portion of the follicle largely determines the shape of the fibre produced'. Class-3 crimp forms or uniplanar waves can also be produced within the model proposed here under similar conditions assumed for class-1 forms. The difference required appears to lie in the detailed structure of the relationship between longitudinal and shear strain for the para- and orthocortical cells. It is intended to present the details of this special case in a separate paper, since it would lengthen this discussion considerably.

It may be concluded, therefore, that the model summarized in the previous section has the capacity to produce all three major classes of crimp form. Apart from predicting the shape or form, any proposed mechanism for crimp must also be capable of interpreting the relationships known to exist between staple-crimp frequency and fibre diameter. These relationships are, however, complex and depend on the level of nutrition and age as well as on genetic factors (Roberts and Dunlop 1957). A comparison of crimp frequency predicted by the mechanism proposed here, with observations, would require a fairly long discussion. It is intended to present the model predictions and comparison later. It will be shown that predictions are consistent with the known dependence of crimp frequency on follicle length (Nay and Johnston 1967) which is related to fibre diameter.

Acknowledgments

I wish to acknowledge the support and advice given by Dr J. L. Black and Mr R. E. Chapman, both of the Division of Animal Production, CSIRO. I also wish to thank Angus and Robertson Publishers and Mr R. E. Chapman for permission to reproduce Figs 10, 11 and 12 from Chapman (1965).

References

- Amad, N., and Lang, W. R. (1957). Ortho-para cortical differentiation in 'anomalous' Merino wool. *Aust. J. Biol. Sci.* **10**, 118-24.
- Auber, L. (1950). The anatomy of follicles producing wool fibres, with special reference to keratinization. *Trans. R. Soc. Edinburgh* **62**, 191-254.
- Balasubramaniam, E., and Whiteley, K. J. (1964). Theoretical configurations of single wool fibres. I. Sine and helical forms. *Aust. J. Appl. Sci.* **15**, 41-52.
- Barker, S. G., and Norris, M. H. (1930). A note on the physical relationships of crimp in wool. *J. Text. Inst.* **21**, T1-17.
- Brown, T. D., and Onions, W. J. (1961). A theory for the development of wool fibre crimp on drying. *J. Text. Inst.* **52**, T101-8.
- Chapman, R. E. (1965). The ovine arrector pili musculature and crimp formation in wool. In 'Biology of the Skin and Hair Growth'. (Eds A. G. Lyne and B. F. Short.) (Angus and Robertson: Sydney.)
- Chapman, R. E. (1971). Cell migration in wool follicles of sheep. *J. Cell. Sci.* **9**, 791-803.
- Chapman, R. E. (1976). Electron microscopic and histochemical features of the formation of the orthocortex and paracortex in wool. Proc. 5th Int. Wool Text. Res. Conf., Aachen 1975. (Ed. K. Ziegler.) Vol. II.
- Chapman, R. E., and Gemmell, R. T. (1971). Stages in the formation and keratinization of the cortex of the wool fiber. *J. Ultrastruct. Res.* **36**, 342-54.
- Downes, A. M., and Sharry, L. F. (1971). Measurement of wool growth and its response to nutritional changes. *Aust. J. Biol. Sci.* **24**, 117-30.
- Fraser, I. E. B. (1964). Studies on the follicle bulb of fibres. 1. Mitotic and cellular segmentation in the wool follicle with reference to ortho- and para-segmentation. *Aust. J. Biol. Sci.* **17**, 521-31.
- Horio, M., and Kondo, T. (1953). Crimping of wool fibres. *Text. Res. J.* **23**, 373-86.
- Jacobs, O. L. R. (1974). 'Introduction to Control Theory.' pp. 218-26. (Clarendon Press: Oxford.)

- Mercer, E. H. (1961). 'Keratin and Keratinization: an Essay in Molecular Biology.' (Pergamon Press: Oxford.)
- Nay, T., and Johnston, H. (1967). Follicle curvature and crimp size in some selected Australian Merino groups. *Aust. J. Agric. Res.* **18**, 833-40.
- Onions, W. J. (1962). 'Wool—An Introduction to its Properties, Varieties, Uses and Production.' (Ernest Benn Ltd: London.)
- Roberts, N. F., and Dunlop, A. A. (1957). Relationship between crimp and fineness in Australian Merinos. *Aust. J. Agric. Res.* **8**, 524-46.
- Rogers, G. E. (1959a). Electron microscopic studies of hair and wool. *Ann. N.Y. Acad. Sci.* **83**, 378-99.
- Rogers, G. E. (1959b). Electron microscopy of wool. *J. Ultrastruct. Res.* **2**, 309-30.
- Rossouw, S. D. (1931). A preliminary study on the relationship between crimp and contour in wool fibres. *J. Text. Inst.* **22**, T374-84.
- Thomas, G. B. (1962). 'Calculus and Analytic Geometry.' (Addison-Wesley: London.)
- Wildman, A. B. (1932). Coat and fibre development in some British sheep. *Proc. Zool. Soc. Lond.* **1932**, 257-85.

Manuscript received 1 April 1980, accepted 24 February 1981

Appendix

Curvature of an Unrestricted Fibre

Consider a fibre which at a certain point along its length is bent with curvature R^{-1} . The cross-section of the fibre at that point is an ellipse (shown in Fig. 9a). The fibre consists of bilateral segments with the paracortex on the inside of the curvature as indicated in Fig. 9b which shows a longitudinal section of the fibre in the plane of the curvature. It is possible to express R in terms of the mechanical properties of the fibre; the properties needed are Young's moduli (E_p , E_o), the longitudinal strain (ε_p , ε_o) and the geometrical distribution of the para- and orthocortex in the cross-section. The expression is obtained by imposing two constraints which must be true if the bent fibre is free of external forces:

- (1) There must be zero net force acting on the cross-section, i.e.

$$\int_{-h}^b \int_{-w}^w S_o \, dx \, dy + \int_{-b}^{-h} \int_{-w}^w S_p \, dx \, dy = 0, \quad (\text{A1})$$

where

$$w = [a^2 - (ay/b)^2]^{\frac{1}{2}},$$

and

$$S_i = E_i[(\varepsilon_i - \varepsilon) + (y+c)]/R, \quad i = p, o$$

c is the point (in the y -direction) at which there is zero longitudinal stress due to bending, and is therefore defined by the condition:

$$\int_{-h}^b \int_{-w}^w E_o(y+c)/R \, dx \, dy + \int_{-b}^{-h} \int_{-w}^w E_p(y+c)/R \, dx \, dy = 0,$$

i.e.

$$E_o[u_o - (h-c)]A_o = E_p[u_p + (h-c)]A_p, \quad (\text{A2})$$

where u_o and u_p are the distances of the centres of gravity in the ortho- and paracortex from the join between these two segments (Fig. 9b). Substituting equation (A2) in equation (A1) yields:

$$E_o(\epsilon_o - \epsilon)A_o = E_p(\epsilon_p - \epsilon)A_p, \tag{A3}$$

which determines ϵ , the longitudinal strain existing in the unbent fibre.

(2) There must be zero net moment about c , acting on the cross-section, i.e.

$$\int_{-h}^b \int_{-w}^w S_o(y+c) dx dy + \int_{-b}^{-h} \int_{-w}^w S_p(y+c) dx dy = 0,$$

$$\int_{-h}^b \int_{-w}^w E_o(\epsilon_o - \epsilon)(y+c) dx dy + \int_{-b}^{-h} \int_{-w}^w E_p(\epsilon_p - \epsilon)(y+c) dx dy$$

$$= -(E_o I_o + E_p I_p)/R, \tag{A4}$$

where I_o and I_p are the second moments of area of the ortho- and paracortex about c . Using equations (A2), (A3) and (A4) the expression for R is:

$$R = (E_o I_o + E_p I_p)/(\epsilon_p - \epsilon_o)E_p A_p[u_p + (h - c)].$$

For a circular fibre with $E_o = E_p$ and $h = 0$ the radius of curvature becomes:

$$R = 3\pi D/16(\epsilon_p - \epsilon_o),$$

where $D = a = b$.

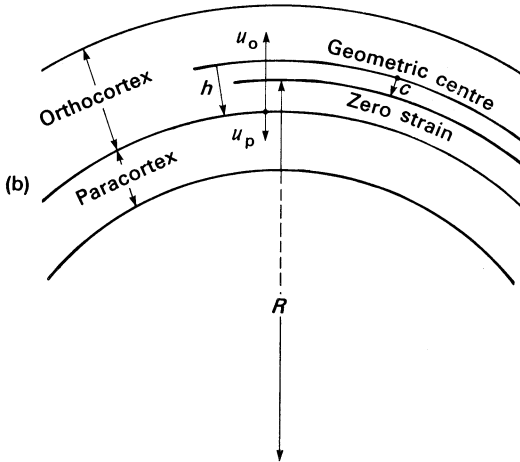
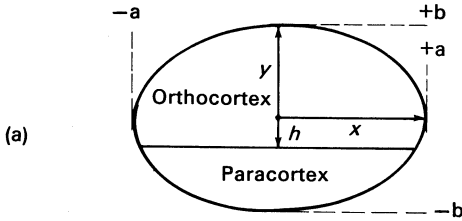


Fig. 9. Cross-section of an elliptical fibre (a) and longitudinal section of a bent fibre through the plane of the bend (b), indicating the dimensions and structure of the fibre.

Curvature of a Restricted Fibre

The analysis of the previous section may be extended to take account of the effect of the inner and outer root sheaths in restricting the curvature of the fibre while it is still within the follicle. Consider the case of a root sheath restricting curvature at a

distance z from the base of the follicle bulb. The effect of both the inner and outer root sheaths will be included explicitly later. The fibre dimensions are the same as those in Fig. 9a. The root sheath surrounds the fibre and its outer boundary is an ellipse defined by $x^2/c^2 + y^2/d^2 = 1$. E_{rs} is Young's modulus for the root sheath.

When condition (1) in the previous section is imposed equation (A1) becomes

$$\theta + 2 \int_{-d}^d \int_{-s}^{-w} E_{rs} [-\varepsilon + (y + c)]/R \, dx \, dy = 0,$$

where θ is the left-hand side of equation (A1) and

$$s = \sqrt{c^2 - (cy/d)^2}.$$

Equation (A2) becomes

$$E_o[u_o - (h - c)]A_o + E_p[-u_p - (h - c)]A_p + E_{rs} A_{rs} C = 0.$$

and equation (A3) now has the form

$$E_o(\varepsilon_o - \varepsilon)A_o + E_p(\varepsilon_p - \varepsilon)A_p - \varepsilon E_{rs} A_{rs} = 0.$$

Imposing condition (2) now yields the following expression for curvature at the point z :

$$R(z) = (E_o I_o + E_p I_p + E_{rs} I_{rs}) / \{E_p \varepsilon_p [u_p + (h - c)]A_p - E_o \varepsilon_o [u_o - (h - c)]A_o\}.$$

In the case where $E_o = E_p = E$ and $h = 0$ this equation reduces to

$$R(z) = (E_o I_o + E_p I_p + E_{rs} I_{rs}) / E u_p A_p (\varepsilon_p - \varepsilon_o). \tag{A5}$$

The effect of two concentric root sheaths, namely, the inner and outer root sheaths, may be included by expressing $E_{rs} I_{rs}$ as a sum of the two root sheaths as follows,

$$E_{rs} I_{rs} = E_{irs} I_{irs} + E_{ors} I_{ors}, \tag{A6}$$

where E_{irs} and I_{irs} are the Young's modulus and second moment of area about c , for the inner root sheath. E_{ors} and I_{ors} are the corresponding quantities for the outer root sheath.

